Generation of Induced Progenitor-like Cells from Mature Epithelial Cells Using Interrupted Reprogramming

Li Guo,[1] Golnaz Karoubi,[1] Pascal Duchesneau,[1] Maria V. Shutova,[2] Hoon-Ki Sung,[3] Peter Tonge,[2]
Christine Bear,[4] Ian Rogers,[2,5,6] Andras Nagy,[2,5,7,*] and Thomas K. Waddell[1,*]

[1]Division of Thoracic Surgery, Toronto General Hospital Research Institute, University Health Network, University of Toronto, Toronto, ON M5G 2C4, Canada
[2]Samuel Lunenfeld Research Institute, Mount Sinai Hospital, Toronto, ON M5T 3H7, Canada
[3]Physiology and Experimental Medicine, Hospital for Sick Children, Toronto, ON M5G 0A4, Canada
[4]Programme in Molecular Structure and Function, Hospital for Sick Children, Toronto, ON M5G 1X8, Canada
[5]Department of Obstetrics and Gynecology, University of Toronto, Toronto, ON M5S 1A1, Canada
[6]Department of Physiology, University of Toronto, Toronto, ON M5S 1A1, Canada
[7]Institute of Medical Science, University of Toronto, Toronto, ON M5S 1A1, Canada
*Correspondence: nagy@lunenfeld.ca (A.N.), tom.waddell@uhn.ca (T.K.W.)
https://doi.org/10.1016/j.stemcr.2017.10.022

SUMMARY

A suitable source of progenitor cells is required to attenuate disease or affect cure. We present an "interrupted reprogramming" strategy to generate "induced progenitor-like (iPL) cells" using carefully timed expression of induced pluripotent stem cell reprogramming factors (Oct4, Sox2, Klf4, and c-Myc; OSKM) from non-proliferative Club cells. Interrupted reprogramming allowed controlled expansion yet preservation of lineage commitment. Under clonogenic conditions, iPL cells expanded and functioned as a bronchiolar progenitor-like population to generate mature Club cells, mucin-producing goblet cells, and cystic fibrosis transmembrane conductance regulator (CFTR)-expressing ciliated epithelium. *In vivo*, iPL cells can repopulate CFTR-deficient epithelium. This interrupted reprogramming process could be metronomically applied to achieve controlled progenitor-like proliferation. By carefully controlling the duration of expression of OSKM, iPL cells do not become pluripotent, and they maintain their memory of origin and retain their ability to efficiently return to their original phenotype. A generic technique to produce highly specified populations may have significant implications for regenerative medicine.

INTRODUCTION

A major block in the critical path of regenerative medicine is the lack of suitable cells to restore function or repair damage. An "ideal" cell for cell therapy will possess the following attributes: (1) non-immunogenic, ideally patient derived; (2) controllable proliferation, allowing directed expansion; and (3) regulatable differentiation, with intrinsic restriction to the appropriate lineage. Primary cultures of somatic cells are not ideal, as they possess limited proliferative capacity and gradually lose their differentiated properties. Endogenous progenitor cells exist in various organs, including the lung (Kim et al., 2005; Rawlins et al., 2009; Rock et al., 2009; Barkauskas et al., 2013; Vaughan et al., 2014; Jain et al., 2015). However, these endogenous progenitor populations are often difficult to identify and isolate, and usually rapidly change *in vitro* (McQualter et al., 2010). In certain pathological conditions, they are limited in number and function (Rock and Königshoff, 2012; Randell, 2006). Therefore, great efforts have been focused on exogenous cell sources. Despite significant progress in generating mature cell types using embryonic stem cells (ESCs) and induced pluripotent stem cells (iPSCs) (Longmire et al., 2012; Mou et al., 2012; Wong et al., 2012; Huang et al., 2013; Firth et al., 2014), some protocols remain limited by low yield and

purity of the desired mature cell types. There is no standardized approach that is applicable to all cell types. Development of personalized therapies based on autologous pluripotent cells remains very expensive. Moreover, for many cell therapy applications the cells will need externally controllable proliferative capacity to maintain homeostasis or respond to injury.

The early steps of reprogramming have recently been the subject of intense investigations (Clancy et al., 2014; Hussein et al., 2014; Lujan et al., 2015; Shakiba et al., 2015). Two papers have documented additional alternative PSC states, specifically the F-class cells described by Tonge et al. (2014), and separate populations expressing identified as either LIN28^{high} or NANOG[high] by Zunder et al. (2015). In this work, we explore the earlier stages of iPSC reprogramming for potentially useful intermediate cell states. Reprogramming is a multistep process comprising initiation, maturation, and stabilization phases (Samavarchi-Tehrani et al., 2010) during continuous expression of exogenous reprogramming factors until the iPSC state is established (Sridharan et al., 2009). There is a rapid induction of cell proliferation during the early phase of reprogramming (Woltjen et al., 2009). Reprogrammed cells retain epigenetic "memory" in the process for significant numbers of doubling, with the cell of origin influencing the molecular epigenetic profile and functional
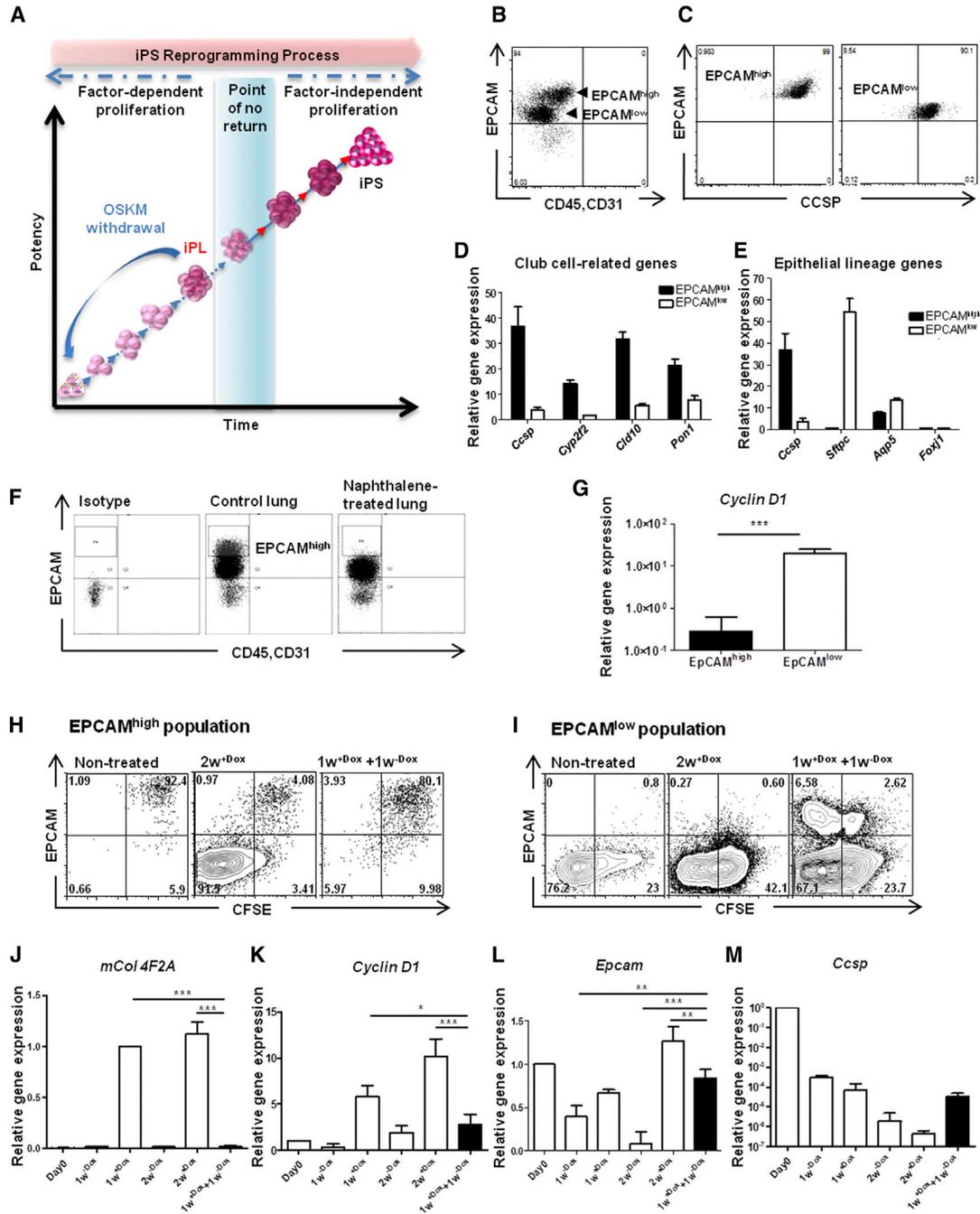
Figure 1. CD31⁻CD45⁻EPCAM^high Epithelial Cells Are a Highly Purified Naphthalene-Sensitive Club Cell Population in which Regulation of Inductive Factors Results in Controlled Proliferation

(A) Schematic graph depicting generation of iPL cells using interrupted reprogramming.

(B) Representative flow-cytometry dot plots showing EPCAM^high and EPCAM^low cells in a parental population of CD31⁻CD45⁻ fresh isolated lung tissue digested cells.

(C–E) Dot plots (C) showing that EPCAM^high cells are exclusive Club cells showing immunoactivity of CCSP. Relative expression of (D) Club cell and (E) other epithelial lineage-related genes to adult lung, comparing fold differences in gene expression in EPCAM^high (solid black bars) and EPCAM^low (open bars) cells.

(F) Representative dot plots comparing EPCAM expression in CD45⁻CD31⁻ freshly isolated lung cells from non-treated and naphthalene-treated mice (n = 3).

differentiation potential of the iPSCs (Kim et al., 2010; Polo et al., 2010; Shipony et al., 2014). Herein, to create therapeutically valuable intermediate cellular products, we took advantage of this early proliferation and speculated that even greater residual epigenetic "memory" exists early in the reprogramming process.

For proof of principle we chose the lung, for which there has been recent progress in the identification of progenitor cells and their hierarchical relationships (Rawlins et al., 2009; Rock et al., 2009; McQualter et al., 2010; Chapman et al., 2011; Barkauskas et al., 2013; Treutlein et al., 2014; Vaughan et al., 2014; Jain et al., 2015), although there remains an unmet need to produce highly purified epithelial populations. For specificity we selected mature Club cells, which possess limited proliferative capacity *in vitro*. Interrupted reprogramming resulted in the generation of large numbers of epithelial progenitor-like cells that demonstrated controlled proliferation and restricted differentiation. This was achieved by optimized, controlled, transient induction of reprogramming factors, turning off their expression prior to reaching independent pluripotency (Figure 1A). We term these cells "induced progenitor-like" (iPL) cells.

Compared with the difficulty of developing directed differentiation protocols for each cell type required, isolation of highly purified populations of adult cells from most organs is already possible using flow-cytometric sorting and cell-culture techniques. These populations, if bestowed with controllable proliferative capacity and limited differentiation potential, would be extremely useful in a variety of regenerative medicine practices, including cell replacement therapy, biohybrid devices, disease modeling, and drug screening for human diseases.

RESULTS

Isolation and Identification of Terminally Differentiated Club Cells

Club cells are secretory cells prominently found in the small bronchioles, identifiable by the presence of Club cell secretory protein (CCSP) (Hackett and Gitlin, 1992). The mature cells have very limited proliferative capacity. After injury, they are replaced from a pool of "variant" Club cells, which are resistant to toxins such as naphthalene. This population

also then serves as progenitors for ciliated and mucous cell populations (Rawlins et al., 2009; Reynolds and Malkinson, 2010). To demonstrate the value of the iPL cell approach, we chose to isolate this terminally differentiated population. Following a modified Club cell isolation protocol (Atkinson et al., 2008), a CD45^{neg}CD31^{neg}EPCAM^{pos} profile defined two distinct epithelial populations, namely EPCAM^{high} and EPCAM^{low} cells (Figure 1B). The EPCAM^{high} population was exclusively Club cells expressing CCSP (Figure 1C) and Claudin10 (Zemke et al., 2008) (Figure S1A), whereas the EPCAM^{low} population contained both Club cells and type II alveolar epithelial (AEC-II) cells (Figures 1C and S1B). Club cell-related genes *Ccsp*, *Cyp2f2*, *Cldn10*, *Aox3*, and *Pon1* were detected within both populations with higher levels in the EPCAM^{high} population (Figures 1D and 1E). Naphthalene administration results in selective loss of mature Club cells (Stripp et al., 1995). To evaluate whether EPCAM^{pos} populations contained functionally different subtypes of Club cells, we compared EPCAM expression in cells isolated from naphthalene-treated and non-treated mice. EPCAM^{high} cells were nearly completely ablated with naphthalene treatment, confirming that they are naphthalene-sensitive, mature Club cells (Figure 1F).

Interrupted Reprogramming Allows OSKM-Dependent Proliferation of EPCAM^{high}-Club Cells

EPCAM^{pos} cells were isolated from R26-rtTA/Col1a1:tetO-4F2A double transgenic mice (Carey et al., 2009) enabling expression of Oct4, Sox2, Klf4, and c-Myc (OSKM) following treatment with doxycycline (Dox). To measure the proliferative response of EPCAM^{pos} cells to inductive factors, we used a specific 2D culture system allowing separation of seeded cells from a feeder population (Kim et al., 2007) (Figure S1C). Control non-treated and Dox-treated EPCAM^{high} and EPCAM^{low} cells were labeled with carboxyfluorescein diacetate succinimidyl ester (CFSE) dye at day 7 and maintained in culture for an additional week in the presence or absence of Dox. Non-treated EPCAM^{high} cells showed very limited proliferation consistent with lower expression of *Cyclin D1*, while Dox treatment resulted in significant proliferation of the majority of cells (Figures 1G and 1H). After treatment with Dox, EPCAM^{high} cells showed significant

(G) Comparison of *Cyclin D1* expression in EPCAM^{high} cells and EPCAM^{low} cells.
(H–M) Representative flow-cytometry dot plots showing CFSE-labeled cells at day 7 (untreated and Dox-treated). EPCAM^{high} cells (H) and EPCAM^{low} cells (I) maintained in feeder-separated semi-supportive culture for an additional 7 days with and without Dox treatment. Control untreated cells were cultured without Dox for the entire 2 weeks. Expression of (J) *mCol4F2A*, (K) *Cyclin D1*, (L) *Epcam*, and (M) *Ccsp*, comparing fold differences in gene expression of EPCAM^{high} freshly isolated (Day0), Dox-treated EPCAM^{high} at 1 week (1w^{+Dox}), and induced cells cultured for an additional week in the presence (2w^{+Dox}) and absence (1w^{+Dox}+1w^{-Dox}) of Dox.
In (B), (C), (F), (H), and (I), data are representative of a minimum of three biological replicates. In (D), (E), (G), and (J)–(M), values are mean ± SD of three independent biological replicates. *p < 0.05; **p < 0.001; ***p < 0.0001.

A

Non-treated | Day7^{+Dox} | Day12^{+Dox} | Day14^{+Dox}

B
H&E

C
DAPI
GFP
EPCAM

D
DAPI 3w^{+Dox} | OCT4 | NANOG | Merge

E
DAPI 5w^{+Dox} | OCT4 | NANOG | Merge

F
DAPI R1-ES | OCT4 | NANOG | Merge
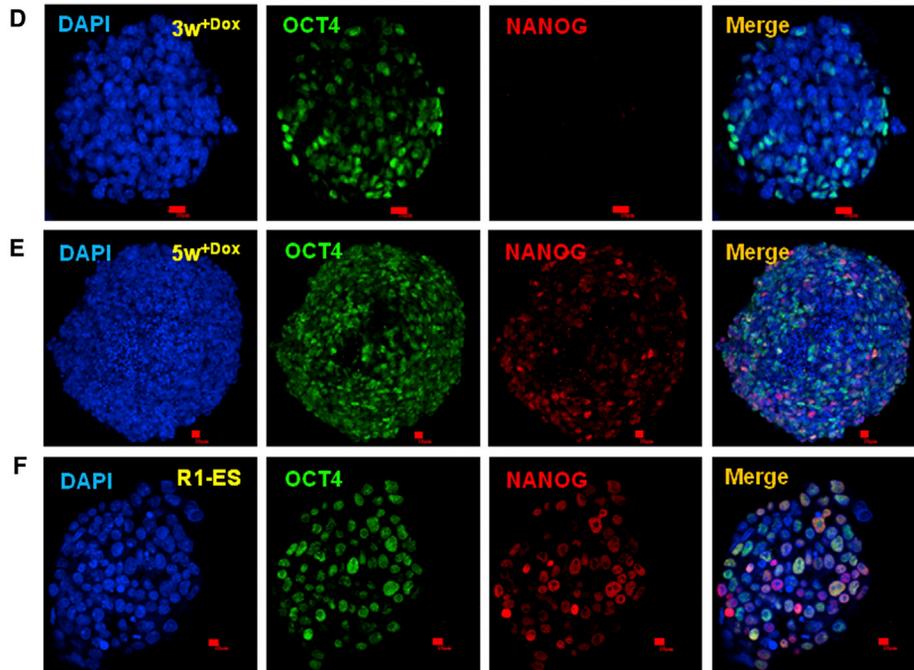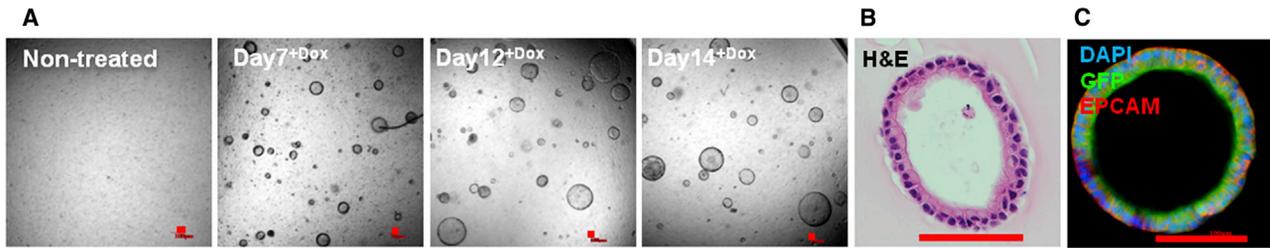
G

Cell type	# of injected cell	# of injection	# of teratoma
R1-ES	0.25 x 10^6	2	2
R1-ES	1.0 x 10^6	2	2
5w^{+Dox}	1.0 x 10^6	4	4
3w^{+Dox}	1.0 x 10^6	4	0
3w^{+Dox}	2.0 x 10^6	4	0

H

Fold change in cell number (Relative to Day0;10^4 cells)
R^2=0.9506
R^2=0.9860
Total number of colonies
2w   3w

I

Cluster A: Utf1, Nanog, Dppa4, Cyp2f2, Aox3, Scgb1a1, Pon1, Muc5ac, Scgb3a2, Muc5b
iPS (log2) vs Day0 (log2)

Cluster B: Utf1, Nanog, Dppa4, Cyp2f2, Muc5b, Muc5ac, Scgb1a1, Aox3, Scgb3a2, Pon1
iPS (log2) vs iPL (log2)

Cluster A 846 Cluster B
1150 42% 44% 1065
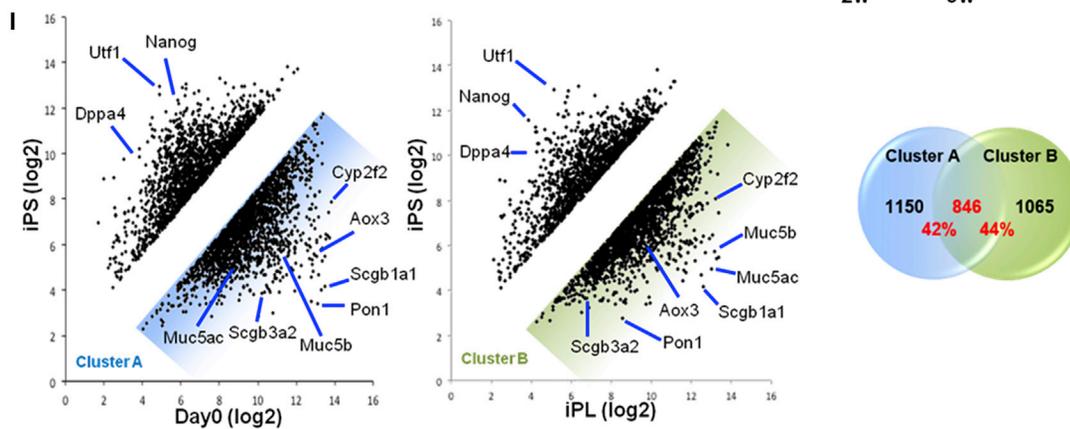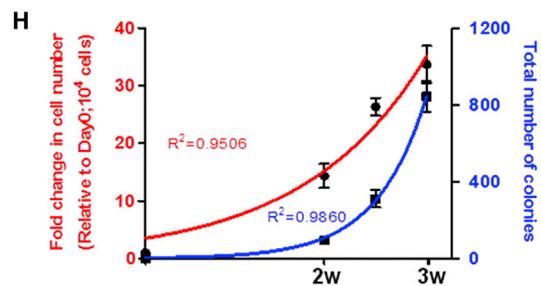
(legend on next page)

upregulation of the *4F2A* construct transgene and *Cyclin D1* (Figures 1J and 1K). Withdrawal of Dox stopped proliferation in the EPCAM^{high} group, while EPCAM^{low} cells continued to proliferate (Figures 1H and 1I). Note the spontaneous loss of EPCAM in the EPCAM^{low} population (Figure 1I). Importantly, *Epcam* and *Ccsp* expression re-emerged following withdrawal of Dox (Figures 1L and 1M). Thus, for these proof-of-principle studies we selected the EPCAM^{high} population, where, as non-proliferative mature Club cells, induced proliferation could be easily distinguished from endogenous proliferation.

Interrupted Reprogramming Results in Clonal Expansion of Quiescent Mature Club Cells without Traversing the Pluripotent State

To better support epithelial cell growth, we cultured EPCAM^{high}-Club cells in Matrigel-based 3D conditions and seeded them on inactivated mouse embryonic fibroblast (MEF) feeder cells prior to Dox treatment. No colonies were formed in the absence of Dox, confirming that native EPCAM^{high} cells lack clonogenic ability. Strikingly, Dox-treated cells exhibited clonogenic growth (Figure 2A) showing epithelial colonies with hollow lumina (Figures 2B and 2C). Time-course analysis indicated that lumen formation occurred as early as day 4 (Figure S2A). This lumen formation occurs at least in part via apoptosis (Grant et al., 2006), marked by caspase-3 expression (Figure S2B), and apical-basal polarization (Martin-Belmonte et al., 2008), as shown by basolateral distribution of EPCAM (Figure 2C) and apical expression of ZO-1 (Figure S2C). Dox induction for 3 weeks (3w^{+Dox}) resulted in suppression of CCSP without activation of the pluripotency marker, NANOG (Figures 2D and 3E). An additional 2 weeks of Dox treatment (5w^{+Dox}) resulted in 22.9% ± 8.3% of colonies becoming NANOG positive (Figure 2E). *In vivo*, 3w^{+Dox} cells

injected into NOD/SCID mice failed to form tumors or teratomas over a 6-month observation period. In contrast, mice developed teratomas 2–3 weeks after injection with either R1 ESCs (Nagy et al., 1993) or 5w^{+Dox} cells (Figures 2G and S2D). Thus, we selected a 3-week induction period during which we achieved the greatest level of expansion without activation of Nanog expression, and hereafter term the 3w^{+Dox} cells Club-iPL cells. During this 3-week period of expansion, cells were serially passaged in the presence of Dox, retained colony-forming potential (Figure 2H, right y axis), and showed an exponential increase in total cell number (∼30-fold expansion) (Figure 2H, left y axis). Microarray analysis of genome-wide transcriptional changes showed that Club-iPL cells have minimal expression of ESC-related genes (e.g., *Nanog*, *Utf1*, *Dapp4*) and maintained significant overlapping expression of Club cell-related genes (Figure 2I).

Interrupted Reprogramming Allows Club-iPL Cells to Return to Their Original Epithelial Phenotype upon Withdrawal of Factors

We assessed the ability of Club-iPL cells to return to their original epithelial phenotype following withdrawal of Dox. Two weeks after withdrawal of Dox (3w^{+Dox}+2w^{-Dox}), cells turned off transgene *4F2A* expression and downregulated *Cyclin D1* (Figures 3A and 3B). Expression of the four individual factors was also significantly downregulated (Figure S3A). Some epithelial genes, such as *Epcam* and *E-cadherin*, were well maintained both with treatment and upon withdrawal of Dox (Figure S3B). CCSP, which was markedly suppressed after 3 weeks of Dox treatment, was expressed at robust levels upon withdrawal of Dox (Figures 3C, 3E, 3F, and 3I). Importantly, NANOG expression was not observed in either Club-iPL cells or 3w^{+Dox}+2w^{-Dox} cells (Figures 3D and 3F) whereas in 4w^{+Dox}+1w^{-Dox} cells, a

Figure 2. Carefully Defined Length of Interrupted Reprogramming Results in Efficient Clonal Expansion of Quiescent Mature Club Cells without Traversing the Pluripotent State *In Vitro*

(A) Light microscopy bright-field images showing the generation of hollow-luminal colonies in the presence of doxycycline in Matrigel-based clonogenic 3D conditions.

(B) H&E staining of sectioned EPCAM^{high} cell-derived colonies under Dox treatment showing hollow-luminal morphology.

(C) Confocal microscopy images of induced colonies derived from GFP-Club cells stained with nuclear stain DAPI (blue), GFP (green), and EPCAM (red).

(D–G) Confocal microscopy images depicting (D) 3-week-induced colonies (3w^{+Dox}) stained with nuclear stain DAPI (blue), OCT4 (green), and NANOG (red). Immunostaining of 5-week-induced colonies (5w^{+Dox}) (E) showing NANOG immunoactivity as that seen in R1 ESCs (F). In an *In vivo* teratoma assay (G), R1 ESCs (positive control), 3w^{+Dox} Club-iPL cells, and 5w^{+Dox} cells were transplanted into NOD/SCID mice (n = 2 mice for each group).

(H) Bulk serial passage of induced colonies during the 3 weeks of induction. Left y axis represents the fold change in total cell number relative to day-0 seeded cells (10,000 cells/well). Right y axis represents the total number of colony-forming units generated. Values are mean ± SD of three independent biological replicates.

(I) Microarray analysis scatterplot showing comparison of iPSCs (generated from EPCAM^{high}-Club cells) with day-0 and Club-iPL cells (left panel); pie charts depicting number of genes overlap in clusters A and B (right panel).

Scale bars, 100 μm (A–C) and 10 μm (D–F).
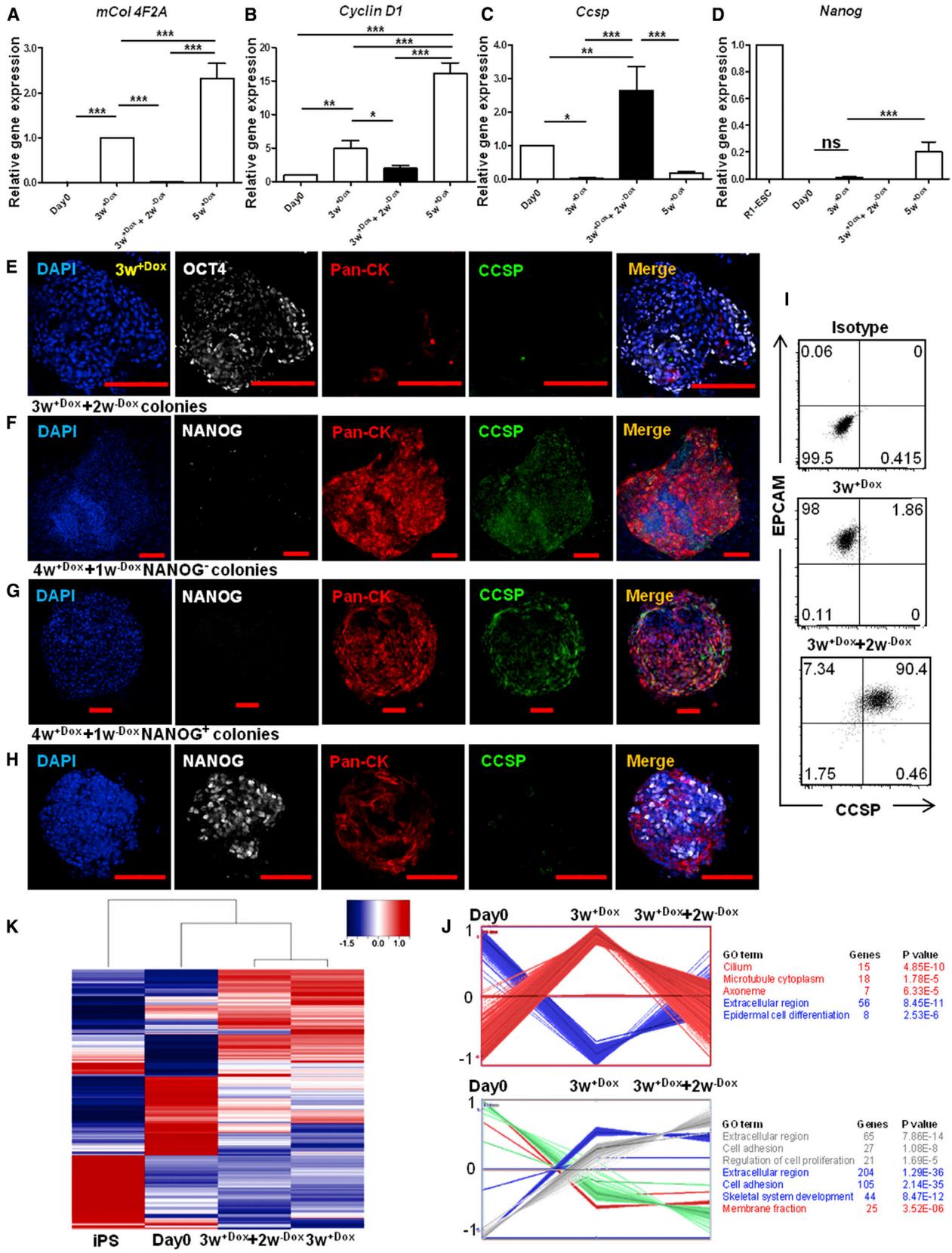
(legend on next page)

few NANOG⁺ colonies were observed (Figures 3G and 3H). Unbiased clustering analysis of the genes with a change ≥3-fold (5,966/24,779 genes) demonstrated that the induced cell groups clustered with the day-0 group (Figure 3J). Further analysis showed that the expression of large numbers of genes temporally changed during Dox-driven expansion of Club cells but returned upon withdrawal of the factors. These gene clusters were enriched for epithelial genes by gene ontology analysis (Figure 3K, top). Other genes demonstrating progressive changes were enriched for metabolism and cell adhesion functions (Figure 3K, bottom), suggestive merely of adaptation to the *in vitro* environment. Figure S3C shows a heatmap of the genes shown in Figure 2I across all four groups.

Interrupted Reprogramming Allows Preservation of Lineage Commitment

To ensure that Club-iPL cells have restricted differentiation, we accessed lineage preference via *in vitro* differentiation assays. Immunostaining of bulk colonies for Pan-CK (endodermal epithelial cells), α-actinin (mesodermal cardiomyocytes), and β-tubulin III (ectodermal neuron cells) demonstrated that Club-iPL cells only developed along an epithelial lineage (Figure 4A). In contrast, cells treated with Dox for 8 weeks ($8w^{+Dox}$), in addition to showing Pan-CK expression (Figure 4B), were able to generate α-actinin⁺ (Figure 4C) and β-tubulin III⁺ cells (Figure 4E). NANOG⁺ undifferentiated cells were also observed (Figure 4D). Moreover, Club-iPL cells exhibited a higher tendency for generation of ciliated cells (β-tubulin IV⁺: 66.7% ± 7.6% of cells) compared with $8w^{+Dox}$ cells (β-tubulin IV⁺: 25.2% ± 5.1% of cells) (Figure 4F). The existence of mixed populations of differentiated cells and undifferentiated cells from the long-term-induced cell group suggests that prolonged induction results in greater divergence from the original lineage and enhanced pluripotency, if not full creation of traditional iPSCs. Lineage commitment at the single-cell level was assessed by culturing independent colonies in three different media

reported to direct differentiation to either neuronal, cardiomyocyte, or epithelial lineages (12 colonies/condition) (Figure S4A). Club-iPL colonies remain committed to an epithelial fate generating Pan-CK⁺ cells but not cardiac troponin T (cTnT)-expressing or β-tubulin III-expressing cells (Figures 4G–4I and S4B).

Club-iPL Cells Function as Multipotent Bronchiolar Progenitor-like Cells

We evaluated the differentiation potential of Club-iPL cells using a two-step protocol (Figure 5A) whereby Club-iPL cells were cultured without Dox for 2 weeks (first step) followed by air-liquid interface (ALI) conditions for 2–3 weeks (second step). The first step of differentiation resulted in upregulation of CCSP (Figures 5B and 5D). Under second-step ALI conditions, iPL cells spontaneously differentiated to MUC5AC-expressing mucin-producing goblet cells (Figure 5E) and β-tubulin IV-expressing ciliated cells (Figure 5F), coinciding with downregulation of *Ccsp* (Figure 5B) and upregulation of *Foxj1* mRNA levels (Figure 5C). Thus, Club-iPL cells can function as multipotent bronchiolar progenitor-like cells, giving rise to Club, goblet, and ciliated cells (Figure 5G).

Club-iPL Cells Are Able to Generate Functional CFTR-Expressing Ciliated Epithelium

Cystic fibrosis transmembrane conductance regulator (CFTR), mainly expressed in ciliated epithelium in the lung, encodes a cyclic AMP (cAMP)-regulated chloride channel that plays a critical role in regulating chloride and water transport. Ciliated epithelium derived from iPL cells expressed functional CFTR protein. We observed that 61.9% ± 6.1% of E-cadherin⁺ cells expressed CFTR, consistent with the formation of functional ciliated epithelium with tight junctions (Figure 6A). We confirmed the apical membrane localization of CFTR while E-cadherin staining was visualized at the lateral membranes (Figure 6B). ALI conditioning resulted in CFTR-expressing cells (Figure 6C). Gene expression analysis of ALI-conditioned

Figure 3. Interrupted Reprogramming Allows EPCAM^high-Club Cell-Derived iPL Cell Colonies to Return to Their Original Epithelial Phenotype upon Factor Withdrawal

(A–H) Expression of (A) the transgene construct *mCol4F2A,* (B) *Cyclin D1*, (C) *Ccsp*, and (D) *Nanog*, as measured by qRT-PCR comparing fold differences in gene expression in freshly isolated cells (Day0), $3w^{+Dox}$ (Club-iPL cells), Club-iPL cells with subsequent 2-week culture in Dox-free medium ($3w^{+Dox}+2w^{-Dox}$), and 5-week-induced cells ($5w^{+Dox}$). Confocal microscopy images of (E) $3w^{+Dox}$ (Club-iPL cells) colonies, (F) colonies obtained from $3w^{+Dox}$ (Club-iPL cells) maintained in culture for 2 weeks in the absence of Dox ($3w^{+Dox}+2w^{-Dox}$), (G) NANOG-negative colonies, and (H) NANOG–positive colonies obtained from 4-week-induced cells ($4w^{+Dox}$) cultured without Dox for 1 subsequent week ($4w^{+Dox}+1w^{-Dox}$), showing cells stained with nuclear stain DAPI (blue), OCT4/NANOG (gray), Pan-CK (red), and CCSP (green).
(I) Representative flow-cytometry dot plots showing expression of EPCAM and CCSP in $3w^{+Dox}$ Club-iPL cells, and iPL cells cultured without Dox for 2 subsequent weeks ($3w^{+Dox}+2w^{-Dox}$).
(J) Unbiased clustering analysis of all genes expressing ≥3-fold change (5,966/24,779).
(K) Self-organizing map analysis of genes that exhibited a >3-fold gene expression difference between cell samples.
For (A)–(D), values are mean ± SD of three independent biological replicates. For (I), data are representative of a minimum of three independent biological replicates. *p < 0.05; **p < 0.001; ***p < 0.0001. Scale bars, 100 μm (E–H).
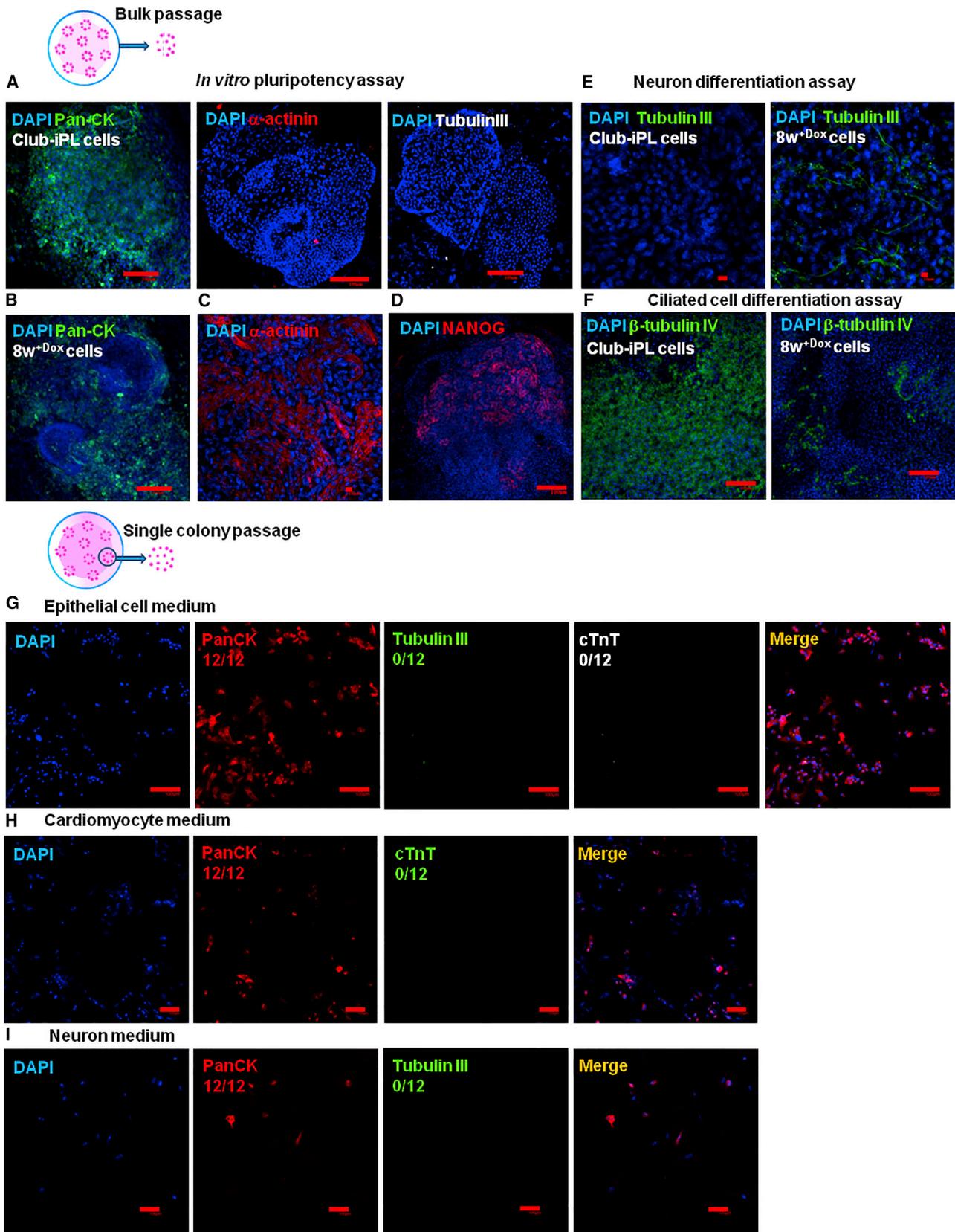
(legend on next page)

cells compared with pre-ALI cells showed a reduction of *Ccsp* expression (Figure 5B) and marked upregulation of *Cftr* (Figure 6D), suggesting the appropriate differentiation of expanded Club cells to CFTR-expressing ciliated cells. An iodide efflux assay measuring cAMP agonist stimulation of the CFTR channel suggests that CFTR seen in Club-iPL-derived ciliated epithelium was functional and appropriately regulated (Figure 6E).

Club-iPL Cells Are Useful in Cell Replacement Therapy for Cystic Fibrosis *In Vivo*

The engraftment of Club-iPL cells into CFTR-deficient epithelium was assessed *in vivo*. For tracking purposes, ROSA26-rtTA/Col1a1: tetO-4F2A double transgenic mice were bred to actin GFP mice and GFP+ Club-iPL cells were delivered to CFTR-knockout mice transtracheally following our previously reported conditioning regimen (Duchesneau et al., 2010, 2017) to augment retention of delivered cells. The engraftment and differentiation capacity of Club-iPL cells in recipient lungs were assessed via staining for ZO-1 or E-cadherin, anti-GFP, and epithelial-type specific markers at 7 and 21 days after cell delivery. CFTR expression in airways of wild-type mice was used as a positive control (Figure 6F) while non-treated and naphthalene-treated CFTR-knockout mice served as negative controls (Figures 6G–6I). Injected GFP cells expressed ZO-1 and E-cadherin, suggestive of their incorporation in recipient epithelium. CFTR-expressing GFP cells were found at days 7 and 21 (Figures 6J and 6K) after iPL cell treatment. Western blotting (Figure 6L) confirmed expression of CFTR protein. A faint band of immature hypoglycosylated CFTR was seen in the untreated CFTR-knockout controls, as expected (in this transgenic animal where the lung is known to have low-level expression of human CFTR) (Zhou et al., 1994). They also increased expression of *Ccsp* and partially restored expression of *Cftr* in CFTR-deficient lungs (Figures 6M and 6N). Consistent with *in vitro* results, CCSP and α-tubulin staining confirmed the differentiation of engrafted Club-iPL cells to Club cells and ciliated cells *in vivo* (Figures S5A–S5E). No SPC+ or AQP5+ GFP+ cells were found, *in vitro* or *in vivo* (data not shown), consistent with restricted commitment to the bronchiolar lineage. To quantify retention, we measured genomic DNA for *GFP* using a standard curve. Donor iPL cells were retained in recipient lungs (Figure S5F) with no significant difference between 7 days (27.8% ± 12.2% of the initial injected cell number) and 21 days (25.8% ± 12.1%) after cell delivery. We also examined the long-term tumorigenicity of iPL cell lines *in vivo* (n = 3). Whole body micro-computed tomography scans taken at 9 months after iPL cell delivery showed no tumors (Figure S5G).

DISCUSSION

A carefully defined period of interrupted reprogramming enabled quiescent mature Club cells to proliferate and start the reprogramming process, but not pass the point of no-return (Nagy and Nagy, 2010), thereby generating large numbers of iPL cells. Upon withdrawal of the inductive factors, iPL cells give rise to CCSP+ Club cells, mucin+ goblet cells, and functional CFTR-expressing ciliated epithelium *in vitro*. They show *in vivo* utility by repopulating CFTR-knockout epithelium after a recipient conditioning regimen. Our results suggest that interrupted reprogramming is not only able to achieve controlled expansion of the selected cell type, but results in the "dedifferentiation" of the cells to a progenitor-like state while preserving the differentiation potential of the parental population to generate a limited range of functional progeny.

Recent advances in the understanding of the mechanisms involved in iPSC reprogramming have demonstrated that "epigenetic memory" found both in human and mouse iPSCs renders them permissive to preferential differentiation to the original lineage (Kim et al., 2010; Bar-Nur et al., 2011; Shipony et al., 2014; De Los Angeles et al., 2015). In our study, we harnessed this "residual epigenetic memory" of the starting cells and generated large numbers of relatively pure progenitor-like populations with intrinsic restriction to the appropriate lineage.

Figure 4. Interrupted Reprogramming Allows Preservation of Lineage Preference and Commitment

(A) Confocal microscopy images of bulk-passaged Club-iPL (3w+Dox) cells, following *in vitro* culture under pluripotency assay conditions. Images show staining for nuclear stain DAPI (blue), Pan-CK (green), α-actinin (red), and tubulin III (gray).

(B–D) Cells induced for 8 weeks (8w+Dox), under *in vitro* pluripotency assay conditions with (B) Pan-CK (green), (C) α-actinin (red), and (D) NANOG (red), respectively.

(E and F) Confocal microscopy images of Club-iPL (3w+Dox) cells and 8-week-induced (8w+Dox) cells under (E) neuron cell differentiation assay conditions showing tubulin III (green) staining and (F) under ALI ciliated cell differentiation conditions showing β-tubulin IV (green) staining.

(G–I) Confocal microscopy images of cells dissociated from single Club-iPL colonies cultured on 10% Matrigel-coated plate under conditions reported for (G) epithelial cells, (H) cardiomyocytes, and (I) neurons. Images show staining for nuclear stain DAPI (blue), Pan-CK (red), tubulin III (green), and cTnT (gray in G, green in H) (n = 12 colonies/each condition).

Scale bars, 10 μm (C and E) and 100 μm (A, B, D, and F–I).
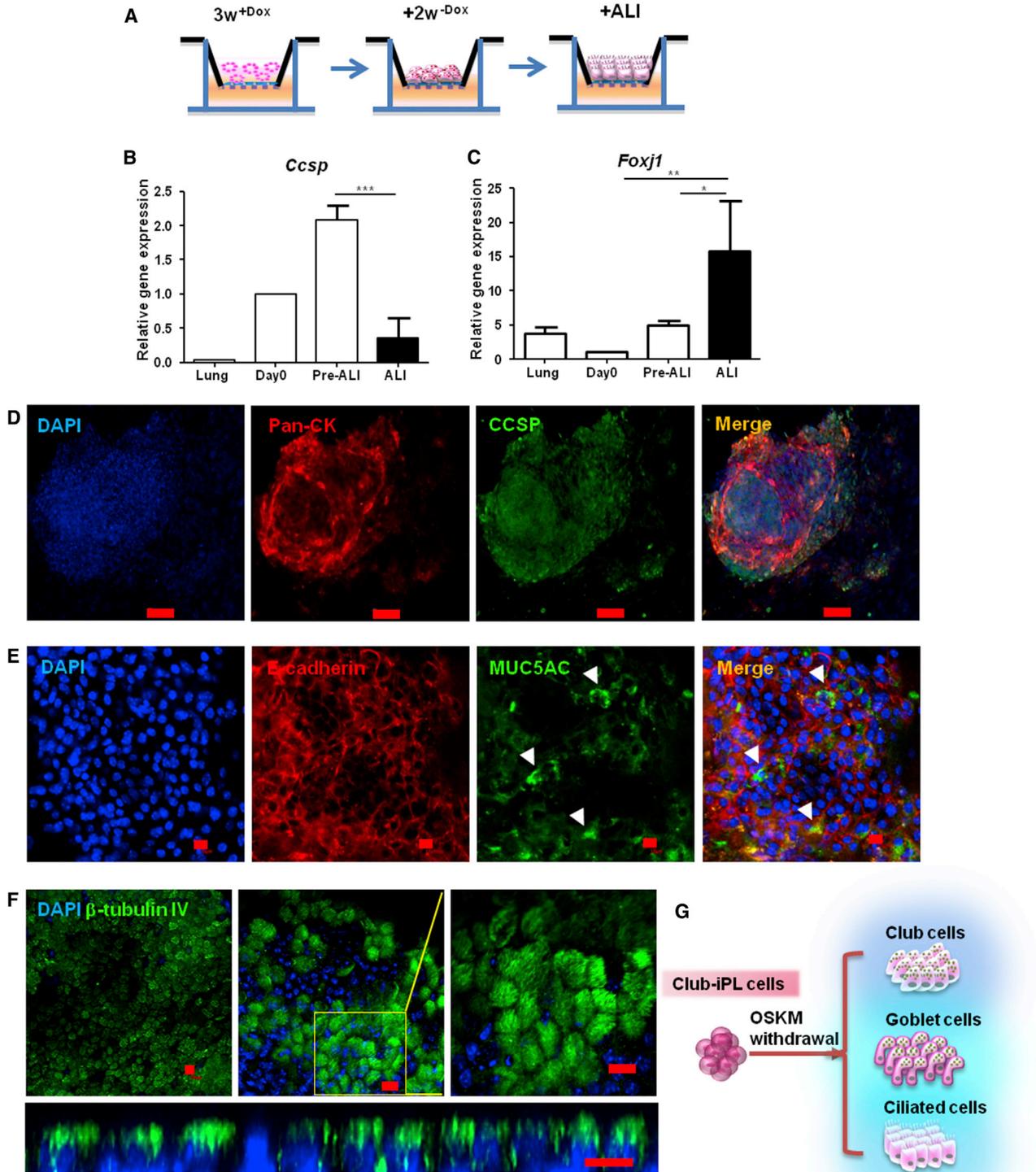
Figure 5. Club-iPL Cells Function as Multipotent Bronchiolar Progenitor-like Cells

(A–C) Schematic graph representing a two-step differentiation protocol (A). Comparison of fold differences in *Ccsp* (B) and *Foxj*1(C) gene expression in adult lung, freshly isolated day-0 cells, $3w^{+Dox}+2w^{-Dox}$ cells (pre-ALI), and cells subsequently cultured in ALI conditions for 2–3 weeks (ALI) by qRT-PCR.

(legend continued on next page)

Despite recent progress in delineating a number of lung progenitor populations and some of their associated markers (Chapman et al., 2011; Jain et al., 2015; Kim et al., 2005; McQualter et al., 2010; Rawlins et al., 2009; Rock et al., 2009; Treutlein et al., 2014; Vaughan et al., 2014), we are still limited in our grasp of the number and characteristics of the lung stem cell hierarchy. After careful comparison using available specific marker expression and microarray data for known lung progenitor populations (Rock et al., 2009; Vaughan et al., 2014), P63-expressing Club-iPL cells do not resemble any *currently identified* progenitors (Figures S6A–S6H). It remains a possibility that they represent a yet unidentified progenitor cell population. Alternatively, transient expression of OSKM in mature lung epithelial cells could result in the generation of a progenitor population not existing in the developing or mature lung—that is, bearing no clear relation to cells in the natural state but nonetheless capable of controlled expansion and differentiation to a limited and appropriate range of progeny. Recent reports highlight the existence of multiple unique cell states en route to pluripotency (Hussein et al., 2014; Tonge et al., 2014; Zunder et al., 2015; Treutlein et al., 2016). Whether or not iPL cells recapitulate a specific developmental stage, enhanced proliferation, and restricted differentiation makes them useful, especially given that this technology can theoretically be applied to almost any cell type that can be isolated and purified.

Superior self-renewal and differentiation capacity of ESCs and iPSCs make both very useful for regenerative medicine, but protocols to generate large numbers of pure, fully differentiated cells are still imperfect. Problems include low differentiation efficiency, heterogeneous final products (Plath and Lowry, 2011; Schwartz et al., 2014), and contamination by potentially tumorigenic undifferentiated cells (Ben-David and Benvenisty, 2011; Tapia and Schöler, 2016). A variety of approaches may overcome these problems, but producing each unique cell that may be desirable will require the development of hundreds of unique protocols. Direct reprogramming through ectopic expression of combinations of specific transcription factors (Caiazzo et al., 2011; Sancho-Martinez et al., 2012) and/or microRNA (Ambasudhan et al., 2011; Leonardo et al., 2012), resulting in direct conversion from one cell type to another, has also been extensively studied. Direct conversion does not require a pluripotent intermediate state and thus may

raise fewer safety concerns. Our interrupted reprogramming strategy similarly avoids pluripotency but may be easier to apply to a broad range of cell types, only requiring that they can be isolated in relative purity.

Recent studies showed *in vitro* differentiation of iPSCs and ESCs to lung epithelium, but were not able to generate large numbers of either Club cells or ciliated cells. Importantly, none of these groups evaluated the *in vivo* contribution of resultant CFTR-expressing cells in an animal model. On the contrary, our iPL cells hold great promise for treating respiratory diseases. Our proof-of-concept *in vivo* studies showed successful retention and incorporation in CFTR-deficient epithelium, with injected iPL cells being able to give rise to both Club cells and ciliated cells.

The significance of this concept results in a number of key issues that need to be addressed. Firstly, our current report suggested that iPL cells are not yet pluripotent. However, our proof-of-principle study was performed using a Dox-inducible polycistronic OSKM system that is known to have a low efficiency for generating bona fide iPSCs, and the absolute safety of this approach requires further evaluation in different OSKM expression systems. Secondly, although we have selected a highly purified population of cells as the starting material, interrupted reprogramming still produces clones that are variable in size, suggesting some degree of heterogeneity in the system. While proliferation during iPL induction seems relatively uniform (Figure 1H, middle panel) and the observed return to phenotype upon Dox withdrawal (Figure 2I) is also homogeneous, potential pluripotency (as suggested by NANOG expression) is more heterogeneous, varying between colonies and among cells within an individual colony after a prolonged induction period (>5 weeks). This will need further exploration but is not surprising, as evidence suggests higher levels of heterogeneity in the early phases of iPSC induction (Lujan et al., 2015; Treutlein et al., 2016; Zunder et al., 2015). There is also some heterogeneity in the differentiation capacity of the Club cells after return from the iPL state, although this can be attributed to the normal biology of Club cells (Rawlins et al., 2009; Reynolds et al., 2000). We also explored the potential of cyclical interrupted reprogramming for even greater expansion of iPL cells *in vitro* (Figures S6I–S6K) and in repopulating injured airway epithelium *in vivo* (Figures S6L–S6P). While significant increases in

(D–F) Confocal microscopy images showing (D) immunostaining of iPL cells after the first step in the differentiation protocol, with nuclear stain DAPI (blue), Pan-CK (red), and CCSP (green); immunostaining of cells after the second step of differentiation protocol with (E) nuclear stain DAPI (blue), E-cadherin (red), and MUC5AC (green) (arrowheads, MUC5AC^{high} cells); and with (F) nuclear stain DAPI (blue) and β-tubulin IV (green).
(G) Schematic graph depicting the differentiation capacity of 3w^{+Dox} (Club-iPL) cells.
For (B) and (C), values are mean ± SD of three independent biological replicates. *p < 0.05; **p < 0.001; ***p < 0.0001.
Scale bars, 10 μm (D–F).
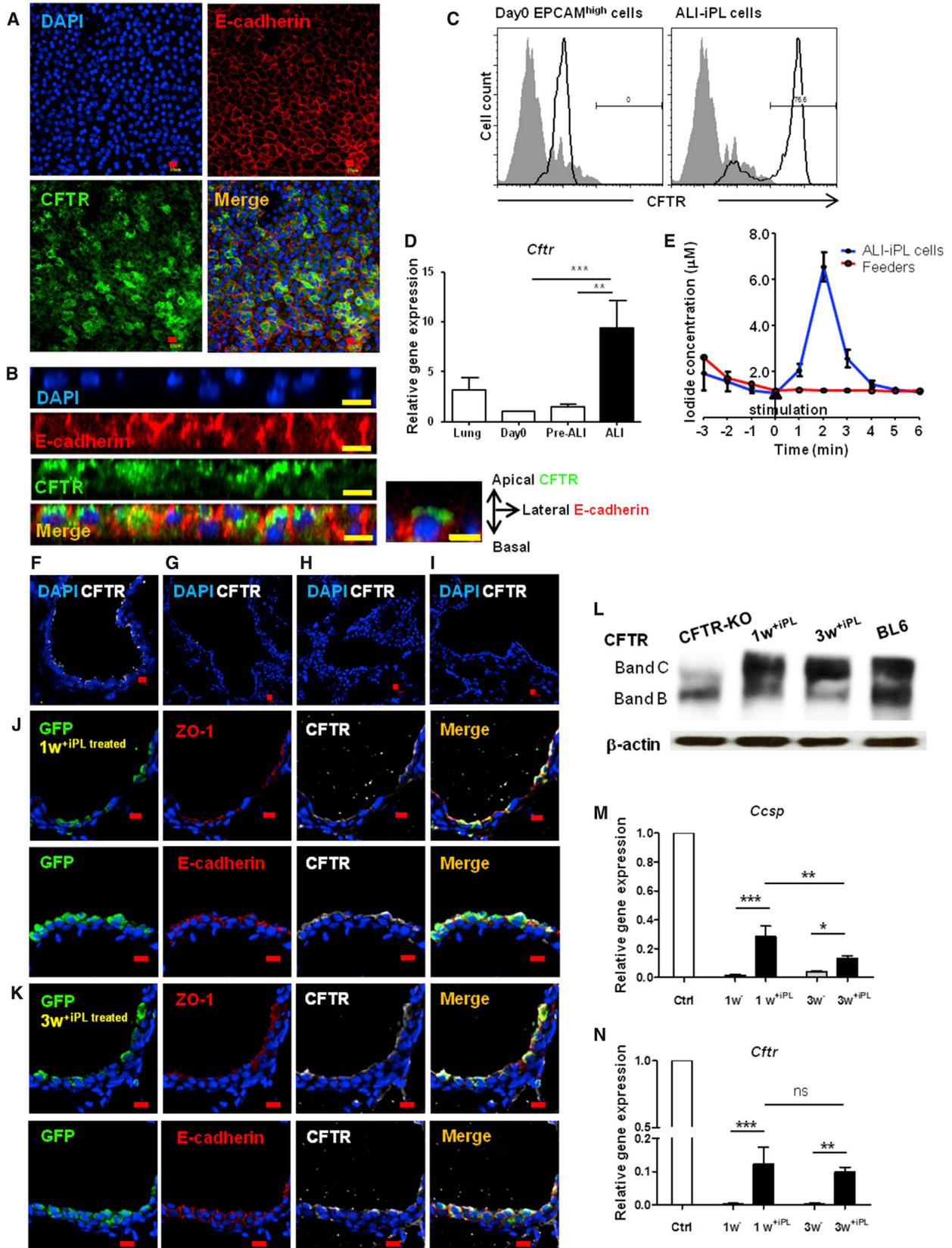
(legend on next page)

cell numbers were seen, the number of cycles resulting in maximal expansion of cells without loss of iPL function remains to be determined. Further refinement is needed to widen the relatively narrow time window during which iPL cell induction and expansion is maximized but before potential factor-independent pluripotency is possible. This may require optimization of exogenous growth factors and/or changes to culture conditions. In addition, the precise requirement for each individual transcription factor remains unknown. Future studies need to be performed to clarify the mechanism underlying the iPL phenomenon and examine whether all factors are necessary. Singovski and colleagues evaluated the effect of transient activation of OSKM, OSK, and M alone (Singovski et al., 2016). While *c-Myc* was important for driving proliferation, only the full four factors resulted in acquisition of a robust "cancer stem cell" phenotype, including increase in colony-forming efficiency. This suggests that the combination of all four factors has downstream effects beyond simply *Myc*-driven proliferation. Whether this observation is analogous to our non-malignant "progenitor-like" population remains to be studied. Finally, regarding therapeutic use, the current data were obtained from Col1a1-4F2A mice and it remains to be shown that this technique can be efficiently applied in human cells. In preliminary studies, we isolated normal human lung epithelial cells containing Club cells from excess tissue remaining from lung transplant donors. Cells were transfected with a polycistronic lentiviral vectors driving Dox-regulatable OSKM. Although the induction conditions require further optimization, Dox-induction resulted in increased cell numbers compared with non-treated native epithelial cells (Figure S6Q). Importantly, consistent with our observation in the mouse system,

Dox-treated cells lost their somatic *CCSP* gene expression but regained it following Dox-withdrawal, suggestive of the ability to return to their original phenotype (Figure S6R). The iPL cell induction process will need to be optimized to obtain maximum expansion and scale-up of cells, but should theoretically benefit from the advances driving iPSC research toward non-integrative, non-viral methods of reprogramming. Theoretically, our iPL concept is broadly applicable and could be extended to other somatic cell types, giving rise to numerous progenitor cell populations. Although future investigations will be needed, these proof-of-concept *in vivo* studies showed that iPL cells hold great promise for treating respiratory diseases by true engraftment as "induced" progenitors.

EXPERIMENTAL PROCEDURES

Naphthalene Administration and Cell Delivery
Naphthalene (>99% pure; Sigma-Aldrich, St Louis, MO) was dissolved in Mazola corn oil and injected as described previously (Stripp et al., 1995). Busulfan (Otsuka America Pharmaceutical, Rockville, MD) was given by intraperitoneal injection 1 day after naphthalene treatment at a dose of 20–50 mg/kg, and donor cells were transplanted the following day (10^6 cells in 50 μL of PBS) transtracheally using sterile gel-loading tips. The mice receiving donor cells were rotated to ensure equal dispersion of cell suspension to both lungs.

Cell Culture
Matrigel-Based iPL Cell Induction
Feeders (MEF) were seeded on 0.1% gelatin coated 24-well transwell filter inserts (Corning) 1 day prior to the addition of epithelial cells. Sorted epithelial cells resuspended in 100 μL of Matrigel

Figure 6. Club-iPL Cells Are Able to Generate Functional CFTR-Expressing Ciliated Epithelium *In Vitro*, which Are Useful as a Component of Cell Replacement Therapy for Cystic Fibrosis *In Vivo*

(A) Confocal microscopy images showing immunostaining of ALI-conditioned iPL cells, with nuclear stain DAPI (blue), E-cadherin (red), and CFTR (green).

(B) Reconstruction of x-z projections of horizontal sections showing nuclear stain DAPI (blue), the apical membrane staining of CFTR (green), and the lateral membrane staining of E-cadherin (red).

(C) Flow-cytometry analysis of CFTR expression in freshly isolated (Day0) cells and ALI-conditioned cells.

(D) Comparison of fold differences in *Cftr* gene expression in adult lung, freshly isolated (Day0) cells, pre-ALI cells, and ALI-conditioned cells.

(E) Iodide efflux assay showing CFTR activity in ALI-iPL cells (blue line) induced by cAMP agonist.

(F–K) Confocal microscopy images of (F) native B57/L6 airway control, (G) native CFTR-KO airway epithelium, and injured airway epithelium of CFTR-KO mice at (H) 1 week and (I) 3 weeks post naphthalene treatment showing nuclear stain DAPI (blue) and CFTR (gray). Confocal microscopy images of iPL cell-treated injured airway sections 1 week (J) and 3 weeks (K) post cell delivery, showing nuclear stain DAPI (blue), GFP (green), ZO-1/E-cadherin (red), and CFTR (gray).

(L) Western blot showing the presence of CFTR protein band appearing at approximately 170 kDa, representative of the complex glycosylated functional form of CFTR in homogenized lung tissue from iPL cell-treated CFTR-knockout injured mice.

(M and N) Expression levels of (M) *Ccsp* and (N) *Cftr* in recipient lungs, as measured by qRT-PCR comparing fold differences in expression in wild-type lungs.

For (C), data are representative of a minimum of three biological replicates. For (D), (E), (M), and (N), values are mean ± SD of three independent biological replicates. *$p < 0.05$; **$p < 0.001$; ***$p < 0.0001$. Scale bars, 10 μm (A, B, and F–K).

(BD Biosciences) prediluted 1:1 (v/v) with epithelial-specific medium were added to MEF-coated 24-well transwell filter inserts in a 24-well tissue culture plate containing 500 μL of epithelial medium for 3–5 days, then replaced with ESC medium containing 1.5 μg/mL doxycycline (Sigma). Medium was replenished three times per week. For bulk passaging, whole cultures were dissociated in collagenase (1 mg/mL; Sigma)/dispase (3 mg/mL; BD Biosciences) in PBS to generate a single-cell suspension. For clonal passaging, single colonies were picked and dissociated.

In Vitro Differentiation Assays

To examine the *in vitro* potential of these cells to differentiate along certain lineages, we performed a variety of differentiation assays. iPL cells induced for 3 weeks were compared with a positive control group consisting of cells exposed to reprogramming factors for 8 weeks.

Air-Liquid Interface Differentiation Assay

Prior to the ALI assay, induced cells were cultured and recovered in ESC medium for 2 weeks. For ALI culture, the ESC medium from the upper chamber was removed to expose cells to the air while medium in the lower chamber was replaced with ALI-specific medium (Lonza). Medium was replenished twice per week and cells were maintained under ALI conditions for 2–3 weeks.

In Vitro Pluripotency Assay

An *in vitro* pluripotency assay to assess the potential of these cells to develop into a variety of cell lineages was performed (Levenberg et al., 2003). In brief, induced cells were dissociated and digested to single-cell suspension and then resuspended in 50% (Matrigel) and 20% fetal bovine serum containing medium supplemented with: activin-A (20 ng/mL), transforming growth factor β1 (2 ng/mL), 10 g/mL insulin, 5 g/mL transferrin, and 300 ng/mL retinoic acid for 2–3 weeks. Lineage differentiation was assessed by immunostaining of pan-cytokeratin, α-actinin, and β-tubulin III.

Neuron Differentiation Assay

To determine the lineage commitment of induced cells, we performed a defined neuron differentiation assay (Millipore) with slight modifications. In brief, 3-week- and >8-week-induced cells from Matrigel cultures were digested to single-cell suspension and differentiated under neuron-specific conditions for 2–3 weeks following the manufacturer's protocol. Generation of neurons was accessed by immunostaining of β-tubulin III.

Microarray and Data Analysis

Total RNA was extracted using an RNeasy kit (Qiagen, Canada). Equal amounts of RNA from three separate samples in each group were used for microarray. Microarray expression profiling using Mouse Gene 2.0 ST chips was performed by The Center for Applied Genomics (The Hospital for Sick Children, Toronto, Canada). Gene ontology term analysis was performed by the DAVID Bioinformatics tool. Self-organizing map analysis of gene expression was performed with the use of the analysis tool MultiExperiment Viewer.

ACCESSION NUMBERS

The microarray data were deposited in the Gene Expression Omnibus (http://www.ncbi.nlm.nih.gov/geo/) under accession number GEO: GSE105775.

REFERENCES

Ambasudhan, R., Talantova, M., Coleman, R., Yuan, X., Zhu, S., Lipton, S.A., and Ding, S. (2011). Direct reprogramming of adult human fibroblasts to functional neurons under defined conditions. Cell Stem Cell *9*, 113–118.

Atkinson, J.J., Adair-Kirk, T.L., Kelley, D.G., deMello, D., and Senior, R.M. (2008). Clara cell adhesion and migration to extracellular matrix. Respir. Res. *9*, 1.

Barkauskas, C.E., Cronce, M.J., Rackley, C.R., Bowie, E.J., Keene, D.R., Stripp, B.R., Randell, S.H., Noble, P.W., and Hogan, B.L.M. (2013). Type 2 alveolar cells are stem cells in adult lung. J. Clin. Invest. *123*, 3025–3036.

Bar-Nur, O., Russ, H.A., Efrat, S., and Benvenisty, N. (2011). Epigenetic memory and preferential lineage-specific differentiation in induced pluripotent stem cells derived from human pancreatic islet beta cells. Cell Stem Cell *9*, 17–23.

Ben-David, U., and Benvenisty, N. (2011). The tumorigenicity of human embryonic and induced pluripotent stem cells. Nat. Rev. Cancer 11, 268–277.

Caiazzo, M., Dell'Anno, M.T., Dvoretskova, E., Lazarevic, D., Taverna, S., Leo, D., Sotnikova, T.D., Menegon, A., Roncaglia, P., Colciago, G., et al. (2011). Direct generation of functional dopaminergic neurons from mouse and human fibroblasts. Nature 476, 224–227.

Carey, B.W., Markoulaki, S., Beard, C., Hanna, J., and Jaenisch, R. (2009). Single-gene transgenic mouse strains for reprogramming adult somatic cells. Nat. Methods 7, 56–59.

Chapman, H.A., Li, X., Alexander, J.P., Brumwell, A., Lorizio, W., Tan, K., Sonnenberg, A., Wei, Y., and Vu, T.H. (2011). Integrin α6β4 identifies an adult distal lung epithelial population with regenerative potential in mice. J. Clin. Invest. 121, 2855–2862.

Clancy, J.L., Patel, H.R., Hussein, S.M.I., Tonge, P.D., Cloonan, N., Corso, A.J., Li, M., Lee, D.-S., Shin, J.-Y., Wong, J.J.L., et al. (2014). Small RNA changes en route to distinct cellular states of induced pluripotency. Nat. Commun. 5, 5522.

De Los Angeles, A., Ferrari, F., Xi, R., Fujiwara, Y., Benvenisty, N., Deng, H., Hochedlinger, K., Jaenisch, R., Lee, S., Leitch, H.G., et al. (2015). Hallmarks of pluripotency. Nature 525, 469–478.

Duchesneau, P., Wong, A.P., and Waddell, T.K. (2010). Optimization of targeted cell replacement therapy: a new approach for lung disease. Mol. Ther. 18, 1830–1836.

Duchesneau, P., Besla, R., Derouet, M.F., Guo, L., Karoubi, G., Silberberg, A., Wong, A.P., and Waddell, T.K. (2017). Partial restoration of CFTR function in cftr-null mice following targeted cell replacement therapy. Mol. Ther. 25, 654–665.

Firth, A.L., Dargitz, C.T., Qualls, S.J., Menon, T., Wright, R., Singer, O., Gage, F.H., Khanna, A., and Verma, I.M. (2014). Generation of multiciliated cells in functional airway epithelia from human induced pluripotent stem cells. Proc. Natl. Acad. Sci. USA 111, E1723–E1730.

Grant, M.R., Mostov, K.E., Tlsty, T.D., and Hunt, C.A. (2006). Simulating properties of in vitro epithelial cell morphogenesis. PLoS Comput. Biol. 2, e129.

Hackett, B.P., and Gitlin, J.D. (1992). Cell-specific expression of a Clara cell secretory protein-human growth hormone gene in the bronchiolar epithelium of transgenic mice. Proc. Natl. Acad. Sci. USA 89, 9079–9083.

Huang, S.X.L., Islam, M.N., O'Neill, J., Hu, Z., Yang, Y.-G., Chen, Y.-W., Mumau, M., Green, M.D., Vunjak-Novakovic, G., Bhattacharya, J., et al. (2013). Efficient generation of lung and airway epithelial cells from human pluripotent stem cells. Nat. Biotechnol. 32, 84–91.

Hussein, S.M.I., Puri, M.C., Tonge, P.D., Benevento, M., Corso, A.J., Clancy, J.L., Mosbergen, R., Li, M., Lee, D.-S., Cloonan, N., et al. (2014). Genome-wide characterization of the routes to pluripotency. Nature 516, 198–206.

Jain, R., Barkauskas, C.E., Takeda, N., Bowie, E.J., Aghajanian, H., Wang, Q., Padmanabhan, A., Manderfield, L.J., Gupta, M., Li, D., et al. (2015). Plasticity of Hopx+ type I alveolar cells to regenerate type II cells in the lung. Nat. Commun. 6, 6727.

Kim, C.F.B., Jackson, E.L., Woolfenden, A.E., Lawrence, S., Babar, I., Vogel, S., Crowley, D., Bronson, R.T., and Jacks, T. (2005). Identification of bronchioalveolar stem cells in normal lung and lung cancer. Cell 121, 823–835.

Kim, S., Ahn, S.E., Lee, J.H., Lim, D.-S., Kim, K.-S., Chung, H.-M., and Lee, S.-H. (2007). A novel culture technique for human embryonic stem cells using porous membranes. Stem Cells 25, 2601–2609.

Kim, K., Doi, A., Wen, B., Ng, K., Zhao, R., Cahan, P., Kim, J., Aryee, M.J., Ji, H., Ehrlich, L.I.R., et al. (2010). Epigenetic memory in induced pluripotent stem cells. Nature 467, 285–290.

Leonardo, T.R., Schultheisz, H.L., Loring, J.F., and Laurent, L.C. (2012). The functions of microRNAs in pluripotency and reprogramming. Nat. Cell Biol. 14, 1114–1121.

Levenberg, S., Huang, N.F., Lavik, E., Rogers, A.B., Itskovitz-Eldor, J., and Langer, R. (2003). Differentiation of human embryonic stem cells on three-dimensional polymer scaffolds. Proc. Natl. Acad. Sci. USA 100, 12741–12746.

Longmire, T.A., Ikonomou, L., Hawkins, F., Christodoulou, C., Cao, Y., Jean, J.C., Kwok, L.W., Mou, H., Rajagopal, J., Shen, S.S., et al. (2012). Efficient derivation of purified lung and thyroid progenitors from embryonic stem cells. Cell Stem Cell 10, 398–411.

Lujan, E., Zunder, E.R., Ng, Y.H., Goronzy, I.N., Nolan, G.P., and Wernig, M. (2015). Early reprogramming regulators identified by prospective isolation and mass cytometry. Nature 521, 352–356.

Martin-Belmonte, F., Yu, W., Rodríguez-Fraticelli, A.E., Ewald, A.J., Werb, Z., Alonso, M.A., and Mostov, K. (2008). Cell-polarity dynamics controls the mechanism of lumen formation in epithelial morphogenesis. Curr. Biol. 18, 507–513.

McQualter, J.L., Yuen, K., Williams, B., and Bertoncello, I. (2010). Evidence of an epithelial stem/progenitor cell hierarchy in the adult mouse lung. Proc. Natl. Acad. Sci. USA 107, 1414–1419.

Mou, H., Zhao, R., Sherwood, R., Ahfeldt, T., Lapey, A., Wain, J., Sicilian, L., Izvolsky, K., Musunuru, K., Cowan, C., et al. (2012). Generation of multipotent lung and airway progenitors from mouse ESCs and patient-specific cystic fibrosis iPSCs. Cell Stem Cell 10, 385–397.

Nagy, A., and Nagy, K. (2010). The mysteries of induced pluripotency: where will they lead? Nat. Methods 7, 22–24.

Nagy, A., Rossant, J., Nagy, R., Abramow-Newerly, W., and Roder, J.C. (1993). Derivation of completely cell culture-derived mice from early-passage embryonic stem cells. Proc. Natl. Acad. Sci. USA 90, 8424–8428.

Plath, K., and Lowry, W.E. (2011). Progress in understanding reprogramming to the induced pluripotent state. Nat. Rev. Genet. 12, 253–265.

Polo, J.M., Liu, S., Figueroa, M.E., Kulalert, W., Eminli, S., Tan, K.Y., Apostolou, E., Stadtfeld, M., Li, Y., Shioda, T., et al. (2010). Cell type of origin influences the molecular and functional properties of mouse induced pluripotent stem cells. Nat. Biotechnol. 28, 848–855.

Randell, S.H. (2006). Airway epithelial stem cells and the pathophysiology of chronic obstructive pulmonary disease. Proc. Am. Thorac. Soc. 3, 718–725.

Rawlins, E.L., Okubo, T., Xue, Y., Brass, D.M., Auten, R.L., Hasegawa, H., Wang, F., and Hogan, B.L.M. (2009). The role of Scgb1a1+ Clara cells in the long-term maintenance and repair of lung airway, but not alveolar, epithelium. Cell Stem Cell *4*, 525–534.

Reynolds, S.D., and Malkinson, A.M. (2010). Clara cell: progenitor for the bronchiolar epithelium. Int. J. Biochem. Cell Biol. *42*, 1–4.

Reynolds, S.D., Hong, K.U., Giangreco, A., Mango, G.W., Guron, C., Morimoto, Y., and Stripp, B.R. (2000). Conditional clara cell ablation reveals a self-renewing progenitor function of pulmonary neuroendocrine cells. Am. J. Physiol. Lung Cell. Mol. Physiol. *278*, L1256–L1263.

Rock, J., and Königshoff, M. (2012). Endogenous lung regeneration: potential and limitations. Am. J. Respir. Crit. Care Med. *186*, 1213–1219.

Rock, J.R., Onaitis, M.W., Rawlins, E.L., Lu, Y., Clark, C.P., Xue, Y., Randell, S.H., and Hogan, B.L.M. (2009). Basal cells as stem cells of the mouse trachea and human airway epithelium. Proc. Natl. Acad. Sci. USA *106*, 12771–12775.

Samavarchi-Tehrani, P., Golipour, A., David, L., Sung, H., Beyer, T.A., Datti, A., Woltjen, K., Nagy, A., and Wrana, J.L. (2010). Functional genomics reveals a BMP-driven mesenchymal-to-epithelial transition in the initiation of somatic cell reprogramming. Cell Stem Cell *7*, 64–77.

Sancho-Martinez, I., Baek, S.H., and Belmonte, J.C.I. (2012). Lineage conversion methodologies meet the reprogramming toolbox. Nat. Cell Biol. *14*, 892–899.

Schwartz, R.E., Fleming, H.E., Khetani, S.R., and Bhatia, S.N. (2014). Pluripotent stem cell-derived hepatocyte-like cells. Biotechnol. Adv. *32*, 504–513.

Shakiba, N., White, C.A., Lipsitz, Y.Y., Yachie-Kinoshita, A., Tonge, P.D., Hussein, S.M.I., Puri, M.C., Elbaz, J., Morrissey-Scoot, J., Li, M., et al. (2015). CD24 tracks divergent pluripotent states in mouse and human cells. Nat. Commun. *6*, 7329.

Shipony, Z., Mukamel, Z., Cohen, N.M., Landan, G., Chomsky, E., Zeliger, S.R., Fried, Y.C., Ainbinder, E., Friedman, N., and Tanay, A. (2014). Dynamic and static maintenance of epigenetic memory in pluripotent and somatic cells. Nature *513*, 115–119.

Singovski, G., Bernal, C., Kuciak, M., Siegl-Cachedenier, I., Conod, A., and Ruiz i Altaba, A. (2016). *In vivo* epigenetic reprogramming of primary human colon cancer cells enhances metastases. J. Mol. Cell Biol. *8*, 157–173.

Sridharan, R., Tchieu, J., Mason, M.J., Yachechko, R., Kuoy, E., Horvath, S., Zhou, Q., and Plath, K. (2009). Role of the murine reprogramming factors in the induction of pluripotency. Cell *136*, 364–377.

Stripp, B.R., Maxson, K., Mera, R., and Singh, G. (1995). Plasticity of airway cell proliferation and gene expression after acute naphthalene injury. Am. J. Physiol. *269*, L791–L799.

Tapia, N., and Schöler, H.R. (2016). Molecular obstacles to clinical translation of iPSCs. Cell Stem Cell *19*, 298–309.

Tonge, P.D., Corso, A.J., Monetti, C., Hussein, S.M.I., Puri, M.C., Michael, I.P., Li, M., Lee, D.-S., Mar, J.C., Cloonan, N., et al. (2014). Divergent reprogramming routes lead to alternative stem-cell states. Nature *516*, 192–197.

Treutlein, B., Brownfield, D.G., Wu, A.R., Neff, N.F., Mantalas, G.L., Espinoza, F.H., Desai, T.J., Krasnow, M.A., and Quake, S.R. (2014). Reconstructing lineage hierarchies of the distal lung epithelium using single-cell RNA-seq. Nature *509*, 371–375.

Treutlein, B., Lee, Q.Y., Camp, J.G., Mall, M., Koh, W., Shariati, S.A.M., Sim, S., Neff, N.F., Skotheim, J.M., Wernig, M., et al. (2016). Dissecting direct reprogramming from fibroblast to neuron using single-cell RNA-seq. Nature *534*, 391–395.

Vaughan, A.E., Brumwell, A.N., Xi, Y., Gotts, J.E., Brownfield, D.G., Treutlein, B., Tan, K., Tan, V., Liu, F.C., Looney, M.R., et al. (2014). Lineage-negative progenitors mobilize to regenerate lung epithelium after major injury. Nature *517*, 621–625.

Woltjen, K., Michael, I.P., Mohseni, P., Desai, R., Mileikovsky, M., Hämäläinen, R., Cowling, R., Wang, W., Liu, P., Gertsenstein, M., et al. (2009). piggyBac transposition reprograms fibroblasts to induced pluripotent stem cells. Nature *458*, 766–770.

Wong, A.P., Bear, C.E., Chin, S., Pasceri, P., Thompson, T.O., Huan, L.-J., Ratjen, F., Ellis, J., and Rossant, J. (2012). Directed differentiation of human pluripotent stem cells into mature airway epithelia expressing functional CFTR protein. Nat. Biotechnol. *30*, 876–882.

Zemke, A.C., Snyder, J.C., Brockway, B.L., Drake, J.A., Reynolds, S.D., Kaminski, N., and Stripp, B.R. (2008). Molecular staging of epithelial maturation using secretory cell-specific genes as markers. Am. J. Respir. Cell Mol. Biol. *40*, 340–348.

Zhou, L., Dey, C.R., Wert, S.E., DuVall, M.D., Frizzell, R.A., and Whitsett, J.A. (1994). Correction of lethal intestinal defect in a mouse model of cystic fibrosis by human CFTR. Science *266*, 1705–1708.

Zunder, E.R., Lujan, E., Goltsev, Y., Wernig, M., and Nolan, G.P. (2015). A continuous molecular roadmap to iPSC reprogramming through progression analysis of single-cell mass cytometry. Cell Stem Cell *16*, 323–337.